General and Comparative Endocrinology 285 (2020) 113264

Contents lists available at ScienceDirect

General and Comparative Endocrinology

journal homepage: www.elsevier.com/locate/ygcen

Expression profiles of types 2 and 3 iodothyronine deiodinase genes in relation to vitellogenesis in a tropical damselfish, *Chrysiptera cyanea*

Sung-Pyo Hur[a], Angka Mahardini[b], Yuki Takeuchi[c,d], Satoshi Imamura[b], Nina Wambiji[b], Dinda Rizky[b], Shingo Udagawa[b], Se-Jae Kim[a], Akihiro Takemura[c,*]

[a] Department of Biology, Jeju National University, 102 Jejudahakro, Ara-1 Dong, Jeju-si, Jeju 63243, Republic of Korea
[b] Graduate School of Engineering and Science, University of the Ryukyus, Nishihara 903-0213, Japan
[c] Department of Chemistry, Biology and Marine Science, Faculty of Science, University of the Ryukyus, Senbaru 1, Nishihara, Okinawa 903-0213, Japan
[d] Okinawa Institute of Science and Technology Graduate University, 1919-1, Onna, Okinawa 904-0495, Japan

ARTICLE INFO

Keywords:
Damselfish
In situ hybridization
Iodothyronine deiodinase
qPCR
Triiodothyronine
Vitellogenesis

ABSTRACT

Thyroid hormone (TH) is involved in regulating the reproduction of vertebrates. Its physiological action in the target tissues is due to the conversion of TH by iodothyronine deiodinases. In this study, we aimed to clone and characterize type 2 (*sdDio2*) and type 3 (*sdDio3*) of the sapphire devil *Chrysiptera cyanea*, a tropical damselfish that undergoes active reproduction under long-day conditions, and to study the involvement of THs in the ovarian development of this species. When the cDNAs of *sdDio2* and *sdDio3* were partially cloned, they had deduced amino acid sequences of lengths 271 and 267, respectively, both of which were characterized by one selenocysteine residue. Real-time quantitative PCR (qPCR) revealed that both genes are highly expressed in the whole brain, and *sdDio2* and *sdDio3* are highly transcribed in the liver and ovary, respectively. *In situ* hybridization analyses showed positive signals of *sdDio2* and *sdDio3* transcripts in the hypothalamic area of the brain. Little change in mRNA abundance of *sdDio2* and *sdDio3* in the brain was observed during the vitellogenic phases. It is assumed that simultaneous activation and inactivation of THs occur in this area because oral administration of triiodothyronine (T3), but not of thyroxine (T4), upregulated mRNA abundance of both genes in the brain. The transcript levels of *sdDio2* in the liver and *sdDio3* in the ovary increased as vitellogenesis progressed, suggesting that, through the metabolism of THs, *sdDio2* and *sdDio3* play a role in vitellogenin synthesis in the liver and yolk accumulation/E2 synthesis in the ovary. Taken together, these results suggest that iodothyronine deiodinases act as a driver for vitellogenesis in tropical damselfish by conversion of THs in certain peripheral tissues.

1. Introduction

The thyroid hormones (THs) thyroxine (T4) and triiodothyronine (T3) play important roles in regulating physiological processes such as growth, morphogenesis, osmoregulation, and reproduction in teleost fish (Cyr and Eales, 1996; Habibi et al., 2012). The synthesis of TH in thyroid follicles is centrally controlled by the hypothalamic–pituitary–thyroid (HPT) endocrine axis, which comprises thyrotropin-releasing hormone (TRH) in the hypothalamus and thyrotropin (TSH) in the pituitary (Blanton and Specker, 2007). Furthermore, specific actions of THs in target tissues are due to the activation and inactivation of intercellular deiodination by iodothyronine deiodinases (Habibi et al., 2012; Jarque and Piña, 2014), and consequent conversion from T4 to T3, a biologically active form of TH, and its specific binding to thyroid hormone receptors (Nelson and Habibi, 2009). To date, three iodothyronine deiodinases, type I (Dio1), type II (Dio2), and type III (Dio3), have been identified in vertebrates (Jarque and Piña, 2014; St Germain and Galton, 1997). Among these, Dio2 and Dio3 are involved in the catalytic activity of outer- and inner-ring deiodination, and mediate the conversion from T4 to T3 and from T3 to 3,3′-diiodothyronine (T2), an inactive metabolite, respectively (Habibi et al., 2012). Thus, it is likely that the intercellular activity of these iodothyronine deiodinases ensures TH action in the target tissues (Cicatiello et al., 2018).

It has been reported that T4 treatment accelerates the vitellogenesis of guppy *Poecilia reticulata* (Lam and Loy, 1985). *In vitro* experiments revealed that co-treatment of gonadotropin with T3 enhanced estradiol-17ß (E2) production from the vitellogenic oocytes of rainbow trout

* Corresponding author.
E-mail address: takemura@sci.u-ryukyu.ac.jp (A. Takemura).

https://doi.org/10.1016/j.ygcen.2019.113264
Received 3 June 2019; Received in revised form 21 August 2019; Accepted 26 August 2019
Available online 27 August 2019

Oncorhynchus mykiss (Cyr and Eales, 1988, 1989) and medaka *Oryzias latipes* (Soyano et al., 1993). Therefore, it is likely that THs are positively involved in endocrine regulation of vitellogenesis in certain fish species through direct action on ovarian follicles (Cyr and Eales, 1996). However, studies using the female goldfish *Carassius auratus* have shown that both T4 and T3 down-regulate the transcript levels of luteinizing hormone (LH) in the pituitary (Yoshiura et al., 1999) and estrogen receptors (ERs) and aromatase in the ovary (Nelson et al., 2010). These results with goldfish seem to imply that THs reduce reproductive activity. Therefore, there is discordance between TH action and reproduction in different fish species. This may be partially due to differences in reproductive modes, as the goldfish is a seasonal spawner, and energy expenditure shifts from reproduction to growth concomitant with an increase in THs after spawning season (Habibi et al., 2012). These insights have been obtained from *in vivo* or *in vitro* experiments with THs, not from molecular studies on iodothyronine deiodinases. Approaches based on these enzymes may be key to understanding the physiological role of THs in reproduction because iodothyronine deiodinases are involved in TH actions in target tissues. Previous studies of these enzymes in fish have focused on metamorphosis (Isorna et al., 2009) and tissue-specific regulation (Isorna et al., 2009; Johnson and Lema, 2011; Klaren et al., 2005; Sambroni et al., 2001; Sanders et al., 1999; Valverde et al., 1997; Van der Geyten et al., 2005; Wambiji et al., 2011a,b).

The sapphire devil *Chrysiptera cyanea* is a reef-associated damselfish that is commonly distributed within the West Pacific region (Myers, 1999). In subtropical waters, this species undergoes seasonal reproduction with long-day preference (Bapary et al., 2009; Bapary and Takemura, 2010). It has been reported that the reproductive activity of this species during the spawning season is influenced by food availability, even if the photoperiod and temperature are within a suitable range for reproduction to continue; limited food supplies suppress oocyte development and spawning frequency, but resumption of food supply leads to restoration of these activities (Bapary et al., 2012). These previous findings raise the hypothesis that nutritional status affects the initiation and termination of ovarian development in this species, and that THs are involved in this process, as certain hormones (e.g., growth hormone, insulin-like growth factor, leptin, and TH) play a role in conveying growth and energetic information to the reproductive endocrine axis (Migaud et al., 2010). In this study, we aimed to clone and characterize cDNAs of *Dio2* (*sdDio2*) and *Dio3* (*sdDio3*) of the sapphire devil. Localization of *sdDio2* and *sdDio3* in the brain was confirmed using *in situ* hybridization, and their transcript levels in the brain by TH administration were measured using real-time quantitative polymerase chain reaction (qPCR). Furthermore, changes in the mRNA abundance of *sdDio2* and *sdDio3* in several tissues were compared between vitellogenic phases.

2. Materials and methods

2.1. Experimental fish

The sapphire devil individuals used in this study were collected using hand nets during daytime low tides from coral reefs around Okinawa, Japan. They had body masses ranging from 1.57 to 3.96 g and total lengths ranging from 4.4 to 5.6 cm. Except for the females used in Experiment 2, most fish were transferred to Sesoko Station, Tropical Biosphere Research Center, University of the Ryukyu, Japan, and kept in tanks (500-liter capacity) with running seawater and aeration under natural photoperiodic conditions. They were fed daily at 10:00 h with commercial pellets (Fry Feed Kyowa C 1000; Scientific Feed Laboratory, Tokyo, Japan) until experimental use. All experiments were carried out in compliance with the Animal Care and Use Committee guidelines of the University of the Ryukyu and regulations for the care and use of laboratory animals in Japan.

For determining the tissue distribution of *sdDio2* and *sdDio3*

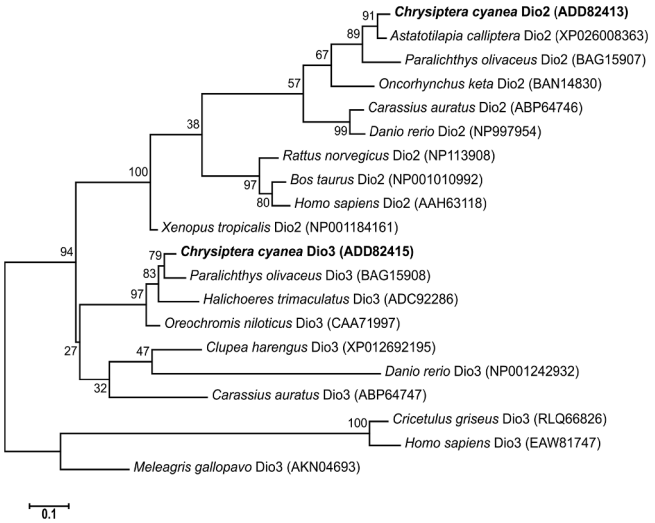

Fig. 1. Phylogenetic tree of amino acid sequences of iodothyronine deiodinases subtypes (sdDio2 and sdDio3). Maximum likelihood analysis with 1000 bootstrap replications was performed to construct the tree. Each value under the node indicates the bootstrap proportion value (maximum proportion value = 100). The scale bar represents the substitution rates per site. Sequences from the sapphire devil (*Chrysiptera cyanea*) are shown in bold.

(Experiment 1), mature females (n = 5) were anesthetized at 12:00 h with 2-phenoxyethanol (Kanto Chemical, Tokyo, Japan). After recording the body mass and total length, they were euthanized by decapitation. Tissues (whole brain, kidney, liver, intestines, muscle, and ovary) were taken, homogenized in 500 µl of TriPure Isolation reagent (Roche Diagnostics, Indianapolis, IN), frozen in liquid nitrogen, and stored at –80 °C. Some brains were fixed in 4% paraformaldehyde for *in situ* hybridization.

We analyzed changes in *sdDio2* and *sdDio3* mRNA abundance in tissues of vitellogenic females (Experiment 2). Mature females (5–8 individuals per month) collected from February to July were immediately sacrificed after anesthetization with 2-phenoxyethanol. After recording their body mass and total length, the whole brain, liver, and ovary were taken, homogenized in 500 µl of TriPure Isolation reagent, frozen in liquid nitrogen, and then stored at –80 °C. Before immersion in TriPure Isolation reagent, the ovary was weighed to calculate the gonadosomatic index [(ovarian mass/body mass) × 100] and cut into small pieces. These were preserved in Bouin's solution for histological observations.

The effect of the administration of T3 and T4 on the mRNA abundance of *sdDio2* and *sdDio3* in the brain was also investigated (Experiment 3). Thyroid hormones (T3 and T4, Sigma-Aldrich, St. Louis, MO) were dissolved in 0.05 M NaOH, diluted to 1 mg/ml with ethanol, and sprayed onto commercial pellets (mg/g diet). For control, vehicle only was sprayed onto the pellets. Immature fish (6 individuals per group) were housed in three aquariums (30-liter capacity) with filtered seawater and aeration under a programmed photoperiod (lights on at 08:00 h, lights off at 18:00 h) and temperature of 25 ± 0.5 °C. They were orally administrated T3-containing pellets (T3-group), T4-containing pellets (T4-group), and control pellets (control group). Feeding was carried out every day at 10:00 h for one week. At the end of the experiment, the fish were anesthetized with 2-phenoxyethanol and sacrificed. After recording the body mass and total length, the whole brain was taken to separate the hypothalamus, which was then frozen in liquid nitrogen and stored at –80 °C until RNA extraction.

2.2. Histological observations

The preserved samples were dehydrated using an ethanol series, underwent permutation with xylene, and were embedded in paraffin

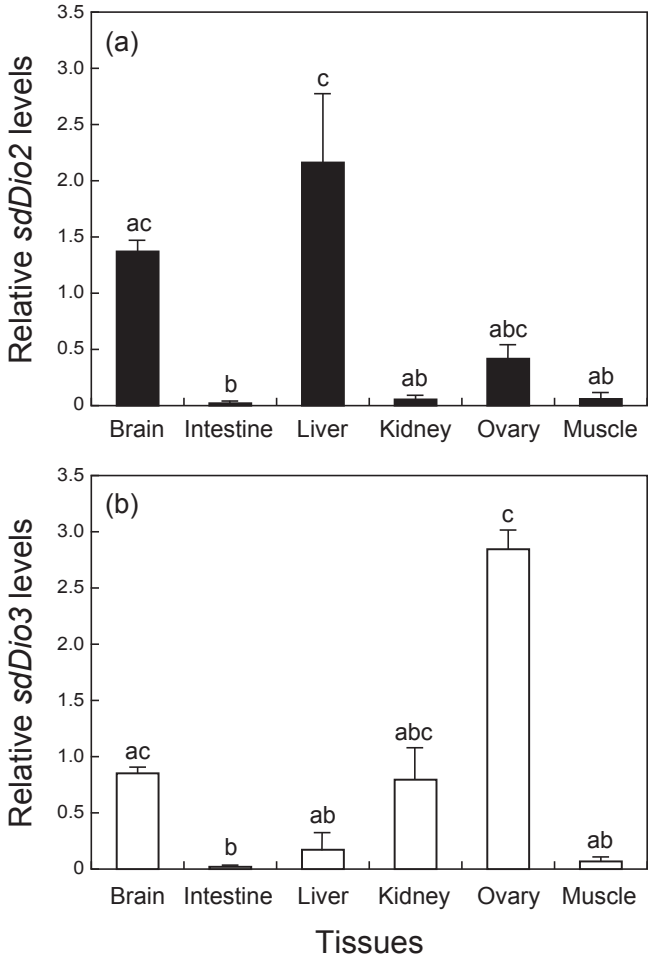

Fig. 2. Expressions of iodothyronine deiodinases in the tissues of the sapphire devil. Tissues (brain, kidney, liver, intestine, muscle, and ovary) were taken from the mature females. Expression levels of *sdDio2* (a) and *sdDio3* (b) were measured using qPCR. The data were normalized by determining the amount of *sdEf1α* mRNA. Each value represents mean ± SEM. Different letters in the figures show significant difference at $P < 0.05$.

(m.p. 56–58 °C; Histologie Merck, Darmstadt, Germany). For histological observation, ovaries were serially sectioned at 5 µm and stained with Mayer's hematoxylin–eosin. Based on previous research (Hoque et al., 1998), oocytes in an ovary were classified into the following stages: peri-nucleolus stage (PNS), oil-droplet stage (ODS), primary yolk stage (PYS), secondary yolk stage (SYS), and tertiary yolk stage (TYS). The ovarian development of the sapphire devil was divided in accordance with a previous report (Imamura et al., 2017).

2.3. Total RNA extraction and cDNA synthesis

Total RNA was extracted from tissues using TriPure Isolation reagent following the manufacturer's protocol. The samples were pretreated with deoxyribonuclease (RT grade; Nippon Gene, Tokyo, Japan) at 37 °C for 15 min to avoid contamination from genomic DNA. The total RNA concentration was investigated using the Thermo Scientific NanoDrop™ 1000 spectrophotometer (Thermo Fisher Scientific, Wilmington, DE). The RNA quality was checked by measuring the A_{260}/A_{280} ratio (1.8–2.0) and by 2% agarose gel electrophoresis with ethidium bromide staining (the clearly detected bands representing *28s* and *18s* ribosomal RNA). The High Capacity cDNA Reverse Transcription Kit (Applied Biosystems, Foster City, CA, USA) was used for cDNA synthesis from 1 µg of total RNA.

2.4. Phylogenetic analyses

Dio2 and *Dio3* cDNAs were cloned from the brain of the sapphire devil. DNA sequences were analyzed using BLASTN and BLASTX (National Center for Biotechnology Information, Bethesda, MD, USA) (http://ncbi.nlm.nih.gov/BLAST) database searches. Multiple alignments for phylogenetic analysis were carried out using the ClustalW method (MEGA 7.0.26; Kumar et al., 2016). The ORF regions were found through https://www.ncbi.nlm.nih.gov/orffinder/. A Phylogenetic tree was constructed using maximum likelihood (ML) method with 1000 bootstrap replications in RAxML version 7.2.6 (Stamatakis, 2006). In addition to this, JTT combined with gamma distribution rates was used as the best fitted model of evolution which determined by MEGA 7.0.26.

2.5. Real-time quantitative PCR (qPCR)

The primer sets for sapphire devil *sdDio2*, *sdDio3*, elongation factor 1 alpha (*sdEf1α*), and β-actin (*sdActin*) are shown in Table S1. The qPCR analysis was performed using the CFX96™ Real Time System (BioRad, Hercules, CA, USA). Each PCR was carried out in a final volume of 10 µl containing 5 µl of 2 × GoTaq qPCR Master Mix (Promega), 0.3 µM of forward and reverse primers, and 2 µl of cDNA template in nuclease-free water. The qPCR cycling conditions were as follows: one cycle at 95 °C for 1 min (denaturation); 40 cycles at 95 °C for 5 s (denaturation), and 60 °C for 1 min (annealing and extension). To ensure the specificity of the PCR amplicons, the temperature of the sample was raised gradually from 60 to 95 °C as the last step of the PCR reaction and the melting curve were analyzed. All qPCR experiments were performed in duplicate. The expression levels were normalized using the ΔΔCt method, with *sdEf1α* or *sdActin* as housekeeping genes. Efficiency (E) values and correlation coefficients (R^2) obtained were as follows: E = 92.5% and R^2 = 0.985 for *sdDio2*; E = 96.7% and R^2 = 0.987 for *sdDio3*; E = 102.5% and R^2 = 0.994 for *sdEf1α*; and E = 96.4% and R^2 = 0.998 for *sdActin*. The use of *sdEf1α* and *sdActin* as internal control genes was preliminary verified by comparing their transcript levels with those of the candidate genes (Fig. S1, Table S1). With the exception of the tissue distribution analysis (Fig. S4), the expression levels of *sdDio2* and *sdDio3* were normalized to that of *sdEf1α* in this study.

2.6. In situ hybridization

The brains embedded in paraffin were sectioned at 7 µm, deparaffinized, washed in phosphate-buffered saline (PBS), permeabilized in TE buffer containing proteinase K (50 µg/mL) for 30 min, and then post-fixed in 4% paraformaldehyde at 4 °C for 10 min. After washing with PBS, sections were acetylated for 20 min with 0.25% acetic anhydride in 0.1 M triethanolamine, pH 8.0, and washed with hybridization buffer (50% formamide, 10% dextran sulfate, 2 × sodium chloride–sodium citrate buffer (SSC), which contained 0.01% salmon sperm DNA).

The hybridization probes of *sdDio2* and *sdDio3*, which amplify fragments of length 243 and 261 bp, respectively (Table S1), were labeled with digoxigenin using a DIG–High Primer DNA Labeling and Detection Starter Kit (Roche Diagnostics GmbH, Mannheim, Germany). Hybridization was carried out in hybridization buffer with 0.1 µg/mL of *sdDio2* or *sdDio3* mRNA probe at 72 °C for 6 h. After hybridization, slides were washed three times for 10 min with 2 × SSC at room temperature.

All procedures for immunological detection of *sdDio2* and *sdDio3* mRNA were carried out using the DIG Nucleic Acid detection kit (Roche Diagnostics GmbH). Sections were washed with Tris-buffered saline (TBS;100 mM Tris-HCl, pH 7.5, containing 150 mM NaCl), blocked with blocking buffer (10% blocking reagent, 90% maleic acid) for 30 min, and then incubated with alkaline–phosphatase-conjugated anti-DIG antibody (1:500) for 60 min. After washing with TBS, sections were incubated overnight with a color solution with 0.16 mg/mL bromo-4-

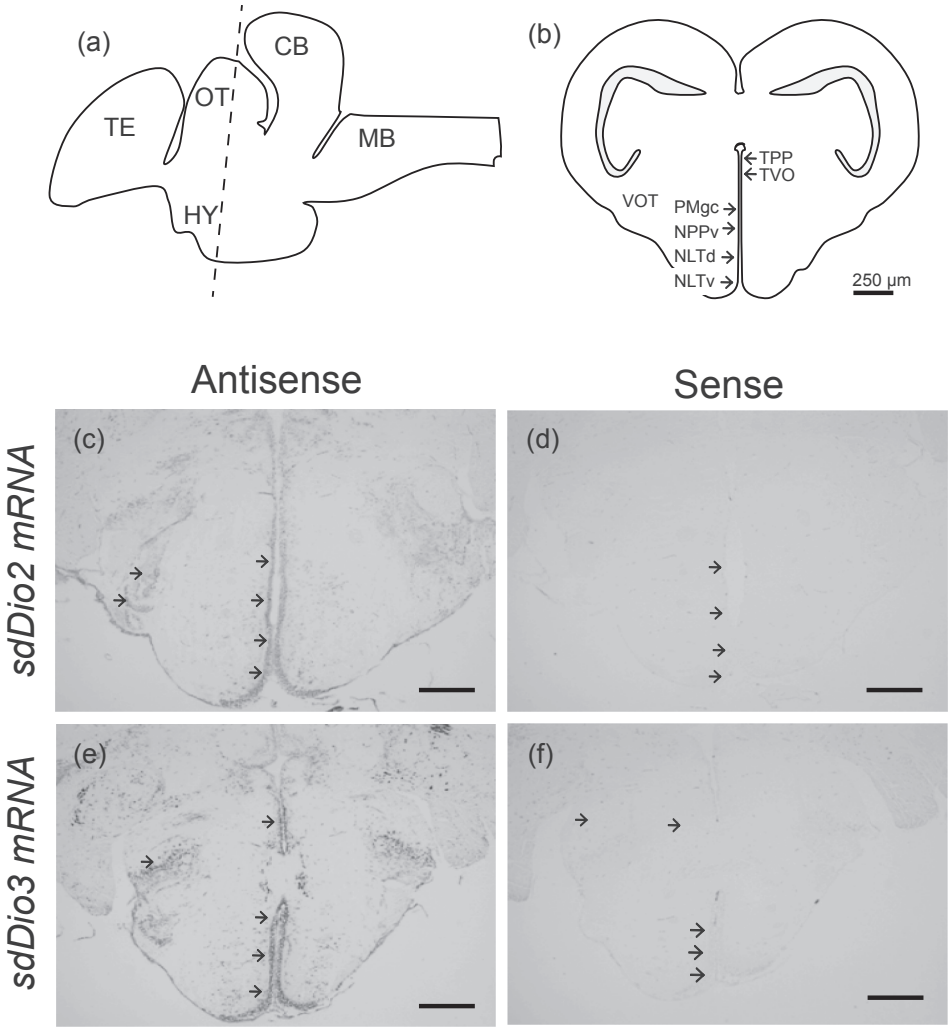

Fig. 3. Detection of iodothyronine deiodinase genes (*sdDio2* and *sdDio3*) in the brain of sapphire devil. The whole brain was fixed in 4% PFA and sectioned at 7 μm. (a) Schematic diagram of the sapphire devil brain (sagittal section). Dot line indicates the plane of sectioning corresponding to B. (b) Diagram showing frontal section of the sapphire devil brain. Signals of *sdDio2* (c and d) and *sdDio3* (e and f) in the mediobasal hypothalamus (MBH) area were detected localized by *in situ* hybridization. Arrows indicates area (positive) with antisense probes (c and e) and identical area (negative) sense probes (d and f). CB: cerebellum; HY: hypothalamus; NLTd: nucleus lateralis tuberis, pars dorsalis; NLTv: ventral part of the lateral tuberal nucleus; NPPv: posterior periventricular nucleus; OT: optic tectum; PMgc: gigantocellular part of the magnocellular preoptic nucleus; PVO: paraventricular organ; MD: medulla oblongata; TE; telencephalon; TPP: periventricular nucleus of the posterior tuberculum; VOT: ventral optic tract. Scale bar = 250 μm.

chloro-3-indolyl-phosphate (BCIP) and 0.33 mg/mL nitro-blue tetrazolium salt (NBT), which were dissolved in 200 mM Tris-HCl, pH 9.2, containing 100 mM NaCl and 50 mM $MgCl_2$. The reaction was stopped by washing sections with 100 mM Tris-HCl, pH 7.5, containing 1 mM EDTA. After washing with 1% DEPC treatment distilled H_2O, sections were mounted using glycerol mounting solution and observed using a light microscope.

2.7. Statistical analyses

All data are presented as the mean ± standard error of the mean (SEM). Kruskal-Wallis and one-way analysis of variance (ANOVA) were carried out to test for significant differences in gene expression between groups (tissue distribution and TH administration, respectively). If significant, the Nemenyi test and Tukey–Kramer honestly significant difference (HSD) test were applied to compare the mean values. Comparisons of the gene expression levels between two vitellogenic stages (EV and LV) were performed using the Mann–Whitney test. In the present study, $P < 0.05$ was accepted as statistically significant.

3. Results

3.1. Cloning and tissue distribution of sapphire devil sdDio2 and sdDio3

The nucleotide sequences of *sdDio2* (Fig. S2) and *sdDio3* (Fig. S3) cDNA (GU583739 and GU583741, respectively) were composed of 816 and 804-bp complete cds with ORF of 271 (ADD82413) and 267 (ADD82415) amino acids, respectively. The Sec residue of *sdDio2* and *sdDio3* was detected in each sequence at 415 and 391 sites, respectively. The amino acid sequences of sdDio2 and sdDio3 were clustered into distinct clades composed of Dio2 and Dio3 and had high identity with that of teleosts and higher vertebrates (Fig. 1).

The qPCR analyses revealed relatively high transcript levels of *sdDio2* and *sdDio3* in the brain. These two iodothyronine deiodinases were differentially transcribed in the liver and ovary; high *sdDio2* and low *sdDio3* transcription was seen in the liver, while opposite transcription was observed in the ovary (Figs. 2 and S4).

3.2. Localization of sdDio2 and sdDio3 mRNA

To localize the *sdDio2* and *sdDio3* mRNA in the hypothalamus, *in situ* hybridization was carried out using a DIG-labeled probe (Fig. 3). Positive signals of *sdDio2* and *sdDio3* were detected in the hypothalamus; *sdDio2* was transcribed in the gigantocellular part of the magnocellular preoptic nucleus (PMgc), posterior periventricular nucleus (NPPv), nucleus lateralis tuberis, pars dorsalis (NLTd), ventral part of the lateral tuberal nucleus (NLTv), and ventral optic tract (VOT) (Fig. 3c), whereas *sdDio3* was found in the NLTd, NLTv, periventricular nucleus of the posterior tuberculum (TPP), paraventricular organ (PVO), and VOT (Fig. 3e). No signal was detected in the same areas of the hypothalamus when the sense primers were used for hybridization (Fig. 3d and f).

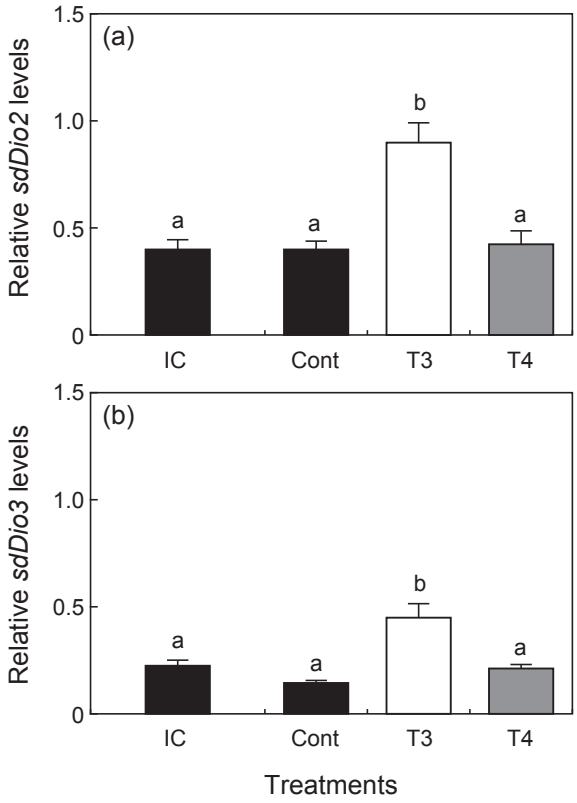

Fig. 4. Effect of thyroid hormone treatments on transcript levels of *sdDio2* and *sdDio3* in the hypothalamus of the sapphire devil. Pellets with thyroid hormones (T3 and T4) and without thyroid hormones (Cont) were orally given to fish for one week. IC shows initial control. The transcription levels of *sdDio2* (a) and *sdDio3* (b) in the hypothalamus were measured using qPCR. The data were normalized by determining the amount of *sdEf1α*. Each value represents mean ± SEM. Different letters in the figures show significant difference at $P < 0.05$.

3.3. Effect of administration of THs on sdDio2 and sdDio3 mRNA abundance in the hypothalamus

THs (T3 and T4) were given to fish to confirm whether this treatment altered the mRNA abundance of *sdDio2* and *sdDio3* in the hypothalamus (Fig. 4). Oral administration of T3, but not T4, resulted in significant increases in transcript levels of *sdDio2* (Fig. 4a) and *sdDio3* (Fig. 4b) in the hypothalamus.

3.4. sdDio2 and sdDio3 mRNA expressions in the hypothalamus in relation to ovarian development

Histological observation revealed that ovaries during the early vitellogenic phase (EV) contained small numbers of oocytes at PYS (Fig. 5a), while those during the late vitellogenic phase (LV) were occupied by well-developed oocytes at TYS (Fig. 5b).

The gonadosomatic index (GSI) was significantly higher during LV (7.25 ± 0.59) than EV (1.27 ± 013) (Fig. 6a). When the transcript levels of *sdDio2* and *sdDio3* were compared between EV and LV, little difference was found between their transcription levels in the hypothalamus (Fig. 6b and d). We also determined the transcript levels of *sdDio2* and *sdDio3* in the liver and ovary, respectively, because *sdDio2* and *sdDio3* were highly expressed in the respective tissues. As a result, the transcription levels of *sdDio2* in the liver were significantly higher during LV than EV (Fig. 6c). A significant increase in the transcription of *sdDio3* was detected in the ovary during LV (Fig. 6e).

4. Discussion

The cDNAs encoding *sdDio2* and *sdDio3* were cloned and characterized to validate experimental approaches to the transcription of these genes. High homology of these iodothyronine deiodinases is supported by our phylogenetic analysis, as *sdDio2* and *sdDio3* were clustered together with their respective enzymes in teleosts. Therefore, the intercellular function of Dio2 and Dio3 is likely to be highly similar between teleosts.

Transcription of *sdDio2* and *sdDio3* was observed in the brain. This implies that the activation and inactivation of intercellular deiodination progress simultaneously in the brain. Evidence that the brain is one major expression site of these genes was obtained in the goldlined spinefoot *Siganus guttatus* (Wambiji et al., 2011a) for *Dio2*, Nile tilapia (Sanders et al., 1999) for *Dio3*, and striped parrotfish *Scarus iseri* (Johnson and Lema, 2011) for both *Dio2* and *Dio3*. *In situ* hybridization results suggest that the *sdDio2* and *sdDio3* signals were observed in the dorsal and ventral sections of the hypothalamus. Notably, kisspeptin receptor genes (*gpr54-1* and *gpr54-2*) were expressed in the diencephalon of the sapphire devil (Imamura et al., 2017). Previous studies have demonstrated that cells expressing kisspeptin mRNA are localized in these regions of zebrafish *Danio rerio* and medaka (Kitahashi et al., 2009), as well as in goldfish (Kanda et al., 2012). Interestingly, intraperitoneal injection of T3 resulted in upregulation of kisspeptin and gonadotropin-releasing hormone (*gnrh1*) mRNA in the brain of male Nile tilapia, suggesting that higher parts of the hypothalamic–pituitary–gonadal (HPG) axis are regulated by THs (Ogawa et al., 2013).

Oral administration of T3 increased the mRNA levels of *sdDio2* and *sdDio3* in the hypothalamus. This implies that the activity of iodothyronine deiodinases in the brain is affected by TH status. On the

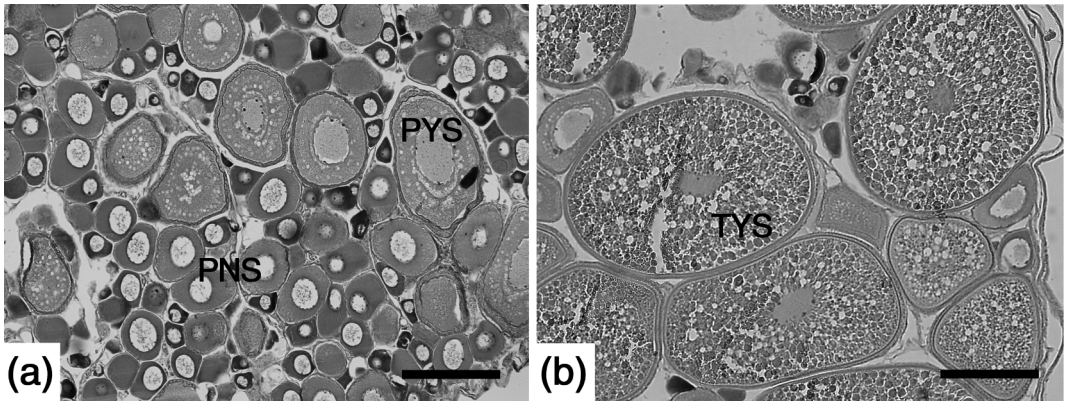

Fig. 5. Ovarian histology of the sapphire devil at different vitellogenic phases. Cross section of early vitellogenesis (a) and late vitellogenesis (b). PNS; peri-nucleolus stage, PYS; primary yolk stage, TYS; tertiary yolk stage. Scale bar = 200 μm.

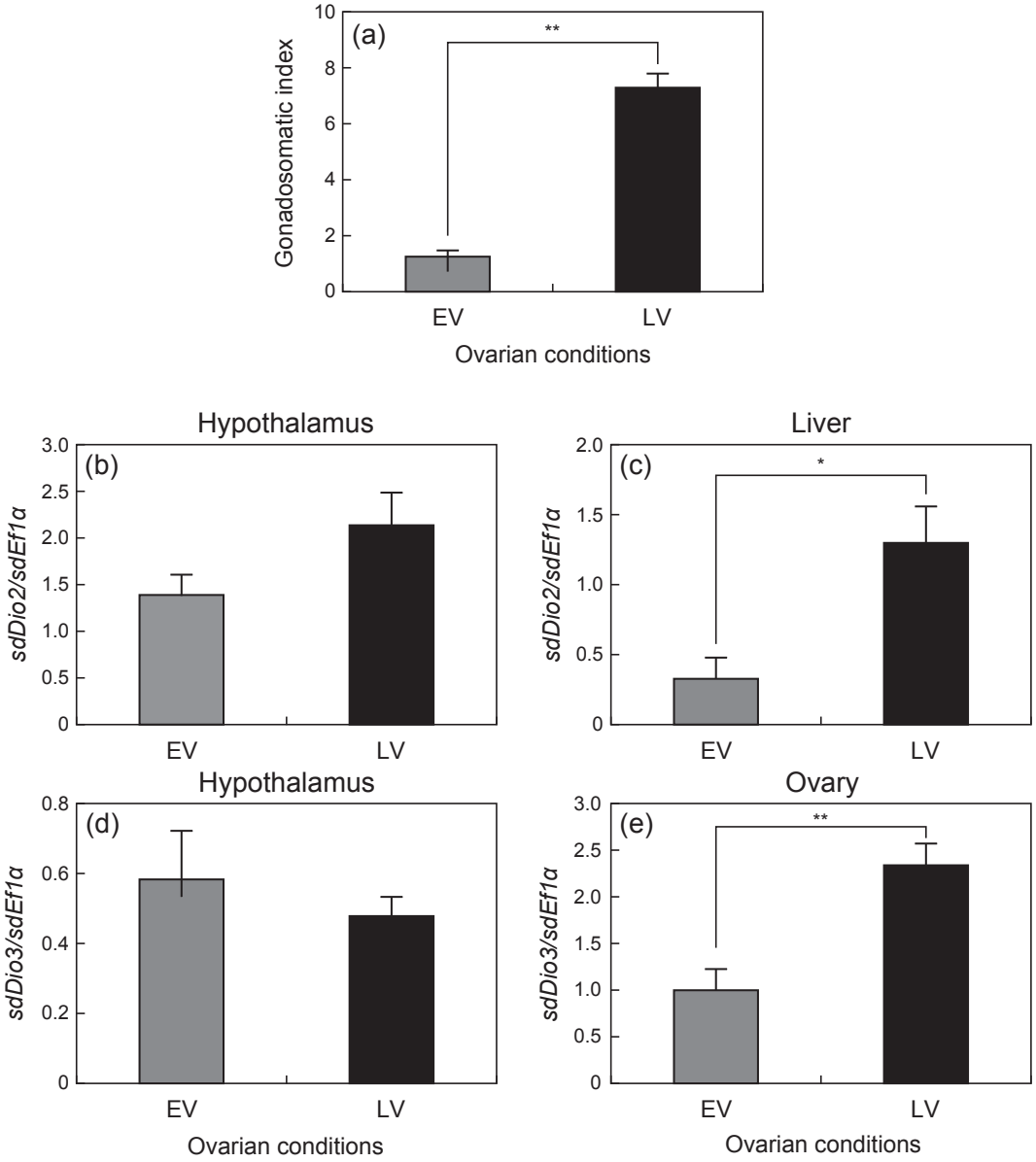

Fig. 6. Comparison of gonadosomatic index (a) and transcript levels of *sdDio2* and *sdDio3* (b–e) in the female sapphire devil during early vitellogenesis (EV) and late vitellogenesis (LV). Tissues (n = 5–8) were collected from the females at EV and LV. Transcript levels of *sdDio2* in the hypothalamus (b) and liver (c) and of *sdDio3* in the hypothalamus (d) and ovary (e) were measured using qPCR. The data were normalized by determining the amount of *sdEf1α*. Each value represents mean ± SEM. Asterisks (* and **) indicate significant difference at $P < 0.05$ and $P < 0.01$, respectively.

other hand, T4 did not alter the transcript levels of either gene in the hypothalamus, suggesting that T4 is centrally and/or peripherally metabolized into inactive forms including reverse-T3 (Habibi et al., 2012). A previous report using the juvenile sea bream *Sparus aurata* revealed that food-delivered propylthiouracil (PTU), an anti-thyroid drug, decreased the transcript levels of *Dio2* and *Dio3* in the brain, but not in the pituitary gland (Morgado et al., 2009). Although the approaches adopted in these two studies (hyperthyroidism for the sapphire devil or hypothyroidism for the sea bream) are different, it is interesting that the activation and inactivation of TH occurred concurrently in the brain. Therefore, it is assumed that the brain is maintained under homeostatic conditions with respect to TH concentration, although we should investigate the hypothalamus to understand this in more detail.

Different transcript profiles of *sdDio2* and *sdDio3* were confirmed in the liver and ovary, with *sdDio2* and *sdDio3* highly transcribed in the liver and ovary, respectively. Habibi et al. (2012) suggested that when circulating T4 reaches the liver and ovary, it is locally metabolized into an active form (T3) and an inactive form (reverse-T3), respectively. A different transcript profile was also noted in the striped parrotfish (Johnson and Chang, 2002). High transcription of *Dio2* was detected in the liver of the rainbow trout (Sambroni et al., 2001) and goldlined spinefoot (Wambiji et al., 2011a). Therefore, it is apparent that, in relation to physiological events, each enzyme specifically functions in its respective peripheral tissues. Previous reports have argued that iodothyronine deiodinases in the liver play a role in the regulation of peripheral T3 status based on observations of mummichog with TH lowered transcript levels of *Dio2* in the liver (García-G et al., 2004). This insight may be supported by experimental evidence that hypothyroidism induced by PTU and methimazole causes upregulation of *Dio2* in the liver of certain teleosts (Johnson and Lema, 2011; Morgado et al., 2009; Van der Geyten et al., 2005). Regarding gonads, the only available results were obtained in the striped parrotfish, in which hyperthyroidism induced by T3 treatment upregulated *Dio2* and *Dio3* in the testis and *Dio2* in the ovary (Johnson and Lema, 2011). It is likely

that changes in enzyme activity are related to testicular development in the rainbow trout, as *Dio2* mRNA peaked during the early spermatogenesis stage (Sambroni et al., 2001).

We compared the *sdDio2* and *sdDio3* transcripts during the early and late vitellogenic phases. The differences between these two phases included the presence of vitellogenic oocytes in the ovary; ovaries during the early vitellogenic phase contained small numbers of vitellogenic oocytes at PYS, whereas those during the late vitellogenic phase were occupied by oocytes at TYS. Therefore, it is expected that the HPG axis is activated and yolk accumulation in developing oocytes actively progresses during the late vitellogenic phase. In fact, the transcript levels of GnRH (*gnrh1*) and gonadotropins [ß-subunit of follicle stimulating hormone (*fshß*) and luteinizing hormone (*lhß*)] increased from the early to the late vitellogenic phase (Imamura, 2017). Both genes were measured in the brain. However, measurement of *sdDio2* and *sdDio3* focused on the liver and ovary, respectively, because high transcription of these genes was observed in the respective peripheral tissues. Our results clearly show that the transcript levels of *sdDio2* increased in the liver, suggesting that T3 in the hepatocytes increased due to the activation of this enzyme. One possibility for the physiological role of elevated T3 is participation in vitellogenin synthesis in hepatocytes. This hypothesis is supported by the fact that when T3 was intraperitoneally injected into goldfish or added to hepatocyte culture medium, the transcript levels of *ERα*, *ERß1*, and *ERß2* were upregulated, and this priming is required for subsequent stimulation of vitellogenin synthesis by E2 (Nelson and Habibi, 2016). Alternatively, elevated *Dio2* may be related to growth-related events, as higher transcript levels of *Dio2* were observed in satiated goldlined spinefoot than in starved specimens (Wambiji et al., 2011b). This conclusion may be supported by the indirect evidence that treatment with T3 stimulates the transcript levels of insulin-like growth factor 1 (*igf1*) in the liver (or hepatocytes) of the Mozambique tilapia *O. mossambicus* (Schmid et al., 2003) and zebrafish (Wang and Zhang, 2011). However, this may be improbable in female sapphire devils undergoing active vitellogenesis, because immersing fish in seawater containing E2 resulted in decreased transcript levels of hepatic *igf1* and *igf2* (Mahardini et al., 2018).

The transcript levels of *sdDio3* increased from the early to late vitellogenic phases, suggesting that, due to the progress of vitellogenesis, T3 is highly inactivated in the ovary. In this regard, T3 treatment lowered the transcript levels of *ERα, ERßI*, and aromatase (*CYP19a*) in goldfish ovaries, suggesting that conversion from testosterone to E2 and E2 action in this tissue is negatively impacted and that energy expenditure is shifted from reproductive to growth efforts (Nelson and Habibi, 2016). The activation of Dio3 toward the late vitellogenic phase may help maintain active vitellogenesis by metabolizing into an inactive form of TH (T2) and reducing the intercellular levels of T3.

It is concluded that iodothyronine deiodinases (*sdDio2* and *sdDio3*) are transcribed differentially between tissues and involved in controlling the seasonal reproduction of the sapphire devil. Previous studies have revealed that the seasonal reproduction of this species is regulated externally by the photoperiod (Bapary et al., 2009; Bapary and Takemura, 2010) and internally by melatonin and dopamine (Badruzzaman et al., 2013, 2015). These factors may be involved in controlling the activities of iodothyronine deiodinases at the transcriptional and post-transcriptional processes because the initiation and termination of seasonal reproduction in fish are influenced by integration of the external and internal factors (Migaud et al., 2010). Further studies are required to clarify the internal and external regulation of these enzymes in seasonal spawners.

Acknowledgement

We gratefully thank to staff of Sesoko Station, Tropical Biosphere Research Center, University of the Ryukyus, Okinawa, Japan, for use of facilities. This study was supported in part by a Grant-in-Aid for Scientific Research (B) (KAKENHI, Grant number 16H05796) from the Japan Society for the Promotion of Science (JSPS) to AT and by a Tongari project under president leadership in the University of the Ryukyus to AT. AM was also very grateful to the Ministry of Education, Culture, Sports, Science and Technology (MEXT), Japan, for making her Ph.D. study by the financial support.

Declaration of Competing interest

The authors have declared no conflict of interest.

Appendix A. Supplementary data

Supplementary data to this article can be found online at https://doi.org/10.1016/j.ygcen.2019.113264.

References

Badruzzaman, M., Bapary, M.A.J., Takemura, A., 2013. Possible roles of photoperiod and melatonin in reproductive activity via changes in dopaminergic activity in the brain of a tropical damselfish, *Chrysiptera cyanea*. Gen. Comp. Endocrinol. 194, 240–247. https://doi.org/10.1016/j.ygcen.2013.09.012.

Badruzzaman, M., Imamura, S., Takeuchi, Y., Ikegami, T., Takemura, A., 2015. Effects of neurotoxin 1-methyl-4-phenyl-1,2,3,6-tetrahydropyridine (MPTP) treatment on ovarian development of the sapphire devil, *Chrysiptera cyanea*. Fish Physiol. Biochem. 41, 61–71. https://doi.org/10.1007/s10695-014-0006-9.

Bapary, M.A.J., Fainuulelei, P., Takemura, A., 2009. Environmental control of gonadal development in the tropical damselfish *Chrysiptera cyanea*. Mar. Biol. Res. 5, 462–469. https://doi.org/10.1080/17451000802644722.

Bapary, M.A.J., Amin, M.N., Takemura, A., 2012. Food availability as a possible determinant for initiation and termination of reproductive activity in the tropical damselfish *Chrysiptera cyanea*. Mar. Biol. Res. 8, 154–162. https://doi.org/10.1080/17451000.2011.605146.

Bapary, M.A.J., Takemura, A., 2010. Effect of temperature and photoperiod on the reproductive condition and performance of a tropical damselfish *Chrysiptera cyanea* during different phases of the reproductive season. Fish. Sci. 76, 769–776. https://doi.org/10.1007/s12562-010-0272-0.

Blanton, M.L., Specker, J., 2007. The hypothalamic-pituitary-thyroid (HPT) axis in fish and its role in fish development and reproduction. Crit. Rev. Toxicol. 37, 97–115. https://doi.org/10.1080/10408440601123529.

Cicatiello, A.G., Di Girolamo, D., Dentice, M., 2018. Metabolic effects of the intracellular regulation of thyroid hormone: old players, new concepts. Front. Endocrinol. 9, 474. https://doi.org/10.3389/fendo.2018.00474.

Cyr, D., Eales, J.G., 1988. *In vitro* effects of thyroid hormones on gonadotropin-induced estradiol-17β secretion by ovarian follicles of rainbow trout, *Salmo gairdneri*. Gen. Comp. Endocrinol. 69, 80–87. https://doi.org/10.1016/0016-6480(88)90055-X.

Cyr, D., Eales, J.G., 1989. T_3 enhancement of *in vitro* estradiol-17β secretion by oocytes of rainbow trout, *Salmo gairdneri*, is dependent on cAMP. Fish Physiol. Biochem. 6, 255–259. https://doi.org/10.1007/BF01875028.

Cyr, D.G., Eales, J.G., 1996. Interrelationships between thyroidal and reproductive endocrine systems in fish. Rev. Fish Biol. Fisher. 6, 165–200. https://doi.org/10.1007/BF00182342.

García-G, C., Jeziorski, M.C., Valverde-R, C., Orozco, A., 2004. Effects of iodothyronines on the hepatic outer-ring deiodinating pathway in killifish. Gen. Comp. Endocrinol. 135, 201–209. https://doi.org/10.1016/j.ygcen.2003.09.010.

Habibi, H.R., Nelson, E.R., Allan, E.R.O., 2012. New insights into thyroid hormone function and modulation of reproduction in goldfish. Gen. Comp. Endocrinol. 175, 19–26. https://doi.org/10.1016/j.ygcen.2011.11.003.

Hoque, M., Takemura, A., Takano, K., 1998. Annual changes in oocyte development and serum vitellogenin level in the rabbitfish *Siganus canaliculatus* (Park) in Okinawa. South. Japan. Fish. Sci. 64, 44–51. https://doi.org/10.2331/fishsci.64.44.

Imamura, S., 2017. Molecular mechanisms of photoregulation on the reproductive activity in the sapphire devil. Doctoral dissertation. University of the Ryukyus, Okinawa.

Imamura, S., Hur, S.-P., Takeuchi, Y., Bouchekioua, S., Takemura, A., 2017. Molecular cloning of kisspeptin receptor genes (*gpr54-1* and *gpr54-2*) and their expression profiles in the brain of a tropical damselfish during different gonadal stages. Comp. Biochem. Physiol. A 203, 9–16. https://doi.org/10.1016/j.cbpa.2016.07.015.

Isorna, E., Obregon, M.J., Calvo, R.M., Vázquez, R., Pendón, C., Falcón, J., Muñoz-Cueto, J.-A., 2009. Iodothyronine deiodinases and thyroid hormone receptors regulation during flatfish (*Solea senegalensis*) metamorphosis. J. Exp. Zool. B 312B, 231–246. https://doi.org/10.1002/jez.b.21285.

Jarque, S., Piña, B., 2014. Deiodinases and thyroid metabolism disruption in teleost fish. Environ. Res. 135, 361–375. https://doi.org/10.1016/j.envres.2014.09.022.

Johnson, J.D., Chang, J.P., 2002. Agonist-specific and sexual stage-dependent inhibition of gonadotropin-releasing hormone-stimulated gonadotropin and growth hormone release by ryanodine: relationship to sexual stage-dependent caffeine-sensitive hormone release. J. Neuroendocrinol. 14, 144–155. https://doi.org/10.1046/j.0007-1331.2001.00756.x.

Johnson, K.M., Lema, S.C., 2011. Tissue-specific thyroid hormone regulation of gene transcripts encoding iodothyronine deiodinases and thyroid hormone receptors in

striped parrotfish (*Scarus iseri*). Gen. Comp. Endocrinol. 172, 505–517. https://doi.org/10.1016/j.ygcen.2011.04.022.
Kanda, S., Karigo, T., Oka, Y., 2012. Steroid sensitive *kiss2* neurones in the goldfish: evolutionary insights into the duplicate kisspeptin gene-expressing neurones. J. Neuroendocrinol. 24, 897–906. https://doi.org/10.1111/j.1365-2826.2012.02296.x.
Kitahashi, T., Ogawa, S., Parhar, I.S., 2009. Cloning and expression of *kiss2* in the zebrafish and medaka. Endocrinology 150, 821–831. https://doi.org/10.1210/en.2008-0940.
Klaren, P.H.M., Haasdijk, R., Metz, J.R., Nitsch, L.M.C., Darras, V.M., Van der Geyten, S., Flik, G., 2005. Characterization of an iodothyronine 5′-deiodinase in gilthead seabream (*Sparus auratus*) that is inhibited by dithiothreitol. Endocrinology 146, 5621–5630. https://doi.org/10.1210/en.2005-0050.
Kumar, S., Stecher, G., Tamura, K., 2016. MEGA7: molecular evolutionary fenetics analysis version 7.0 for bigger datasets. Mol. Biol. Evol. 33, 1870–1874. https://doi.org/10.1093/molbev/msw054.
Lam, T.J., Loy, G.L., 1985. Effect of L-thyroxine on ovarian development and gestation in the viviparous guppy, *Poecilia reticulata*. Gen. Comp. Endocrinol. 60, 324–330. https://doi.org/10.1016/0016-6480(85)90330-2.
Mahardini, A., Yamauchi, C., Takeuchi, Y., Rizky, D., Takekata, H., Takemura, A., 2018. Changes in mRNA abundance of insulin-like growth factors in the brain and liver of a tropical damselfish, *Chrysiptera cyanea*, in relation to seasonal and food-manipulated reproduction. Gen. Comp. Endocrinol. 269, 112–121. https://doi.org/10.1016/j.ygcen.2018.09.001.
Migaud, H., Davie, A., Taylor, J.F., 2010. Current knowledge on the photoneuroendocrine regulation of reproduction in temperate fish species. J. Fish Biol. 76, 27–68. https://doi.org/10.1111/j.1095-8649.2009.02500.x.
Morgado, I., Campinho, M.A., Costa, R., Jacinto, R., Power, D.M., 2009. Disruption of the thyroid system by diethylstilbestrol and ioxynil in the sea bream (*Sparus aurata*). Aquat. Toxicol. 92, 271–280. https://doi.org/10.1016/j.aquatox.2009.02.015.
Myers, R.F., 1999. Micronesian reef fishes: a comprehensive guide to the doral reef fishes of Micronesia. Coral Graphics, Barrigada, Guam.
Nelson, E.R., Habibi, H.R., 2009. Thyroid receptor subtypes: structure and function in fish. Gen. Comp. Endocrinol. 161, 90–96. https://doi.org/10.1016/j.ygcen.2008.09.006.
Nelson, E.R., Habibi, H.R., 2016. Thyroid hormone regulates vitellogenin by inducing estrogen receptor alpha in the goldfish liver. Mol. Cell. Endocrinol. 436, 259–267. https://doi.org/10.1016/j.mce.2016.08.045.
Nelson, E.R., Allan, E.R.O., Pang, F.Y., Habibi, H.R., 2010. Thyroid hormone and reproduction: regulation of estrogen receptors in goldfish gonads. Mol. Reprod. Dev. 77, 784–794. https://doi.org/10.1002/mrd.21219.
Ogawa, S., Ng, K.W., Xue, X., Ramadasan, P.N., Sivalingam, M., Li, S., Levavi-Sivan, B., Lin, H., Liu, X., Parhar, I.S., 2013. Thyroid hormone upregulates hypothalamic *kiss2* gene in the male Nile tilapia, *Oreochromis niloticus*. Front. Endocrinol. 4, 184. https://doi.org/10.3389/fendo.2013.00184.
Sambroni, E., Gutieres, S., Cauty, C., Guiguen, Y., Breton, B., Lareyre, J.-J., 2001. Type II iodothyronine deiodinase is preferentially expressed in rainbow trout (*Oncorhynchus mykiss*) liver and gonads. Mol. Reprod. Dev. 60, 338–350. https://doi.org/10.1002/mrd.1096.
Sanders, J.P., Van der Geyten, S., Kaptein, E., Darras, V.M., Kühn, E.R., Leonard, J.L., Visser, T.J., 1999. Cloning and characterization of type III iodothyronine deiodinase from the fish *Oreochromis niloticus*. Endocrinology 140, 3666–3673. https://doi.org/10.1210/en.140.8.3666.
Schmid, A.C., Lutz, I., Kloas, W., Reinecke, M., 2003. Thyroid hormone stimulates hepatic IGF-I mRNA expression in a bony fish, the tilapia *Oreochromis mossambicus*, in vitro and in vivo. Gen. Comp. Endocrinol. 130, 129–134. https://doi.org/10.1016/s0016-6480(02)00577-4.
Soyano, K., Saito, T., Nagae, M., Yamauchi, K., 1993. Effects of thyroid hormone on gonadotropin-induced steroid production in medaka, *Oryzias latipes*, ovarian follicles. Fish Physiol. Biochem. 11, 265–272. https://doi.org/10.1007/BF00004574.
St Germain, D.L., Galton, V.A., 1997. The deiodinase family of selenoproteins. Thyroid 7, 655–668. https://doi.org/10.1089/thy.1997.7.655.
Stamatakis, A., 2006. RAxML-VI-HPC: maximum likelihood-based phylogenetic analyses with thousands of taxa and mixed models. Bioinformatics 22, 2688–2690. https://doi.org/10.1093/bioinformatics/btl446.
Valverde, C., Croteau, W., Lafleur, G.J., Orozco, A., Germain, D.L., 1997. Cloning and expression of a 5'-iodothyronine deiodinase from the liver of *Fundulus heteroclitus*. Endocrinology 138, 642–648. https://doi.org/10.1210/endo.138.2.4904.
Van der Geyten, S., Byamungu, N., Reyns, G.E., Kühn, E.R., Darras, V.M., 2005. Iodothyronine deiodinases and the control of plasma and tissue thyroid hormone levels in hyperthyroid tilapia (*Oreochromis niloticus*). J. Endocrinol. 184, 467–479. https://doi.org/10.1677/joe.1.05986.
Wambiji, N., Park, Y.-J., Park, J., Kim, S.-J., Hur, S.-P., Takeuchi, Y., Takemura, A., 2011b. Expression patterns of type II and III iodothyronine deiodinase genes in the liver of the goldlined spinefoot, *Siganus guttatus*. Fish. Sci. 77, 301–311. https://doi.org/10.1007/s12562-011-0330-2.
Wambiji, N., Park, Y.-J., Kim, S.-J., Hur, S.-P., Takeuchi, Y., Takemura, A., 2011a. Expression of type II iodothyronine deiodinase gene in the brain of a tropical spinefoot, *Siganus guttatus*. Comp. Biochem. Physiol. A 160, 447–452. https://doi.org/10.1016/j.cbpa.2011.03.023.
Wang, Y., Zhang, S., 2011. Expression and regulation by thyroid hormone (TH) of zebrafish IGF-I gene and amphioxus IGFl gene with implication of the origin of TH/IGF signaling pathway. Comp. Biochem. Physiol. A 160, 474–479. https://doi.org/10.1016/j.cbpa.2011.08.005.
Yoshiura, Y., Sohn, Y.C., Munakata, A., Kobayashi, M., Aida, K., 1999. Molecular cloning of the cDNA encoding the β subunit of thyrotropin and regulation of its gene expression by thyroid hormones in the goldfish, *Carassius auratus*. Fish Physiol. Biochem. 21, 201–210. https://doi.org/10.1023/A:1007884527397.